Negative autoregulation linearizes the dose–response and suppresses the heterogeneity of gene expression

Dmitry Nevozhay[a,1], Rhys M. Adams[a,1], Kevin F. Murphy[b,2], Krešimir Josić[c], and Gábor Balázsi[a,3]

[a]Department of Systems Biology, The University of Texas M. D. Anderson Cancer Center, Houston, TX 77054; [b]Department of Biomedical Engineering, Center for BioDynamics and Center for Advanced Biotechnology, Boston University, Boston, MA 02215; and [c]Department of Mathematics, University of Houston, Houston, TX 77204

Edited by Charles R Cantor, Sequenom Inc., San Diego, CA, and approved January 30, 2009 (received for review October 2, 2008)

Although several recent studies have focused on gene autoregulation, the effects of negative feedback (NF) on gene expression are not fully understood. Our purpose here was to determine how the strength of NF regulation affects the characteristics of gene expression in yeast cells harboring chromosomally integrated transcriptional cascades that consist of the yEGFP reporter controlled by (*i*) the constitutively expressed tetracycline repressor TetR or (*ii*) TetR repressing its own expression. Reporter gene expression in the cascade without feedback showed a steep (sigmoidal) dose–response and a wide, nearly bimodal yEGFP distribution, giving rise to a noise peak at intermediate levels of induction. We developed computational models that reproduced the steep dose–response and the noise peak and predicted that negative autoregulation changes reporter expression from bimodal to unimodal and transforms the dose–response from sigmoidal to linear. Prompted by these predictions, we constructed a ''linearizer'' circuit by adding TetR autoregulation to our original cascade and observed a massive (7-fold) reduction of noise at intermediate induction and linearization of dose–response before saturation. A simple mathematical argument explained these findings and indicated that linearization is highly robust to parameter variations. These findings have important implications for gene expression control in eukaryotic cells, including the design of synthetic expression systems.

gene expression noise | gene networks | linearizer | negative feedback | synthetic biology

Genetically identical cells may be very different in their protein content (1–7) because of stochastic biochemical events underlying gene expression (8, 9), random partitioning of molecules during cell division (10), or different cellular responses to environmental factors (11). This heterogeneity is commonly known as ''gene expression noise,'' and can be either disadvantageous and subject to reduction (12) or beneficial and evolutionarily maintained (13, 14) depending on the biological role of the affected pathways.

Because essentially all genes are parts of transcriptional networks (15), the characteristics of gene expression depend on regulatory motifs present in network topology (16). For example, negative autoregulation is abundant in gene regulatory networks (17) and possibly subject to evolutionary selection (16, 18) because of its ability to reduce gene expression noise (19–21) to speed up gene response times (22), to induce oscillatory gene expression (23, 24), or to reduce the metabolic cost of protein production by the minimization of mRNA usage (18). Despite these findings, the effects of negative feedback (NF) on gene expression are not fully understood. For example, it was suggested that NF alters the shape of the dose–response curve in transcriptional cascades (22, 25, 26), but this effect has never been explored in detail. Such knowledge is vital for the rational design and characterization of increasingly complex transcriptional networks via bottom-up approaches in synthetic biology (27–30).

Our goal was to determine how NF regulation affects the characteristics of gene expression in synthetic transcriptional cascades. We first constructed a TetR-based transcriptional cascade with no feedback in *Saccharomyces cerevisiae* and measured the noise and mean of gene expression at various inducer concentrations. Based on the experimentally measured dose–response, we estimated the biochemical reaction rates and developed a computational model that reproduced the experimentally observed sigmoidal dose–response and noise peak at intermediate levels of induction. The computational model predicted that introducing negative autoregulation into the cascade reduces the heterogeneity of reporter gene expression and linearizes the dose–response before saturation. We verified these predictions by gene expression measurements in a ''linearizer'' gene circuit built by introducing TetR autoregulation into the original transcriptional cascade. Additional gene constructs using different TetR-repressible promoters indicate that this gene circuit is highly robust in producing a linear dose–response and eliminating gene expression heterogeneity at a wide range of inducer concentrations.

Results

Transcriptional Cascade Without Autoregulation. We built a negative-regulatory (NR) gene circuit consisting of chromosomally integrated, separate regulator and reporter parts (Fig. 1*A*). The regulator part of this cascade was the TetR repressor (31) expressed constitutively from the native yeast *GAL1* promoter (P_{GAL1}) in the presence of galactose. The DNA-binding activity of the TetR repressor can be controlled through the extracellular concentration of anhydrotetracycline (ATc) that associates with TetR and blocks its binding to target promoters, thereby enabling the expression of target genes. The reporter part of the NR cascade consisted of the *yEGFP* gene under the control of the $P_{GAL1\text{-}D12}$ promoter (9, 14, 32), which can be repressed by TetR binding to 2 *tet*O_2 sites downstream from the TATA box.

We measured reporter (*yEGFP*) expression means at increasing ATc concentrations across yeast cell populations using flow cytometry and observed a sigmoidal (nonlinear) dose–response, with a steep increase at intermediate induction levels (Fig. 2*A*). The gene expression noise (measured as the coefficient of variation; standard deviation divided by the mean) also peaked at intermediate levels of ATc (50–90 ng/mL), whereas it diminished at low and high levels of ATc (Fig. 2*C*), as observed previously (9, 32). Analysis of population-distribution histo-

Author contributions: D.N., R.M.A., and G.B. designed research; D.N., R.M.A., K.J., and G.B. performed research; K.F.M. contributed new reagents/analytic tools; D.N., R.M.A., and G.B. analyzed data; and D.N., R.M.A., K.J., and G.B. wrote the paper.

The authors declare no conflict of interest.

This article is a PNAS Direct Submission.

Freely available online through the PNAS open access option.

[1]D.N. and R.A. contributed equally to this work.

[2]Present address: Division of Genetics, Department of Medicine, Brigham and Women's Hospital and Harvard Medical School, Boston, MA 02115.

[3]To whom correspondence should be addressed. E-mail: gbalazsi@mdanderson.org.

This article contains supporting information online at www.pnas.org/cgi/content/full/0809901106/DCSupplemental.

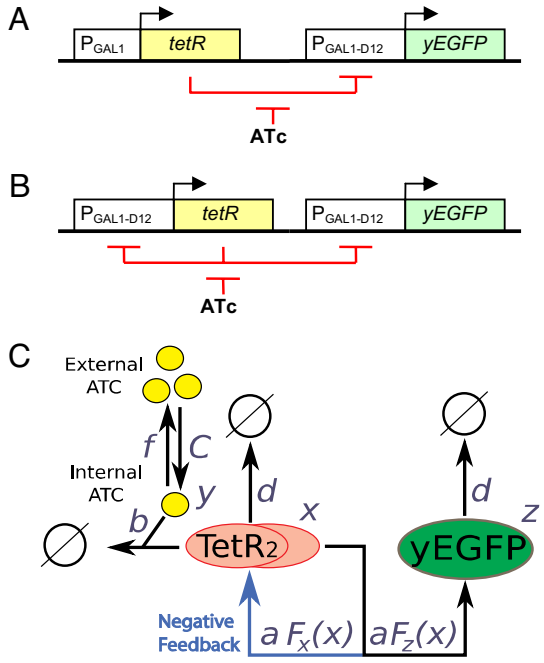

Fig. 1. Diagram of the gene constructs and the corresponding simplified model scheme. (*A*) NR cascade, consisting of the *yEGFP* reporter and the constitutively expressed *tetR* repressor. (*B*) Cascade with NF, consisting of the *yEGFP* reporter and the *tetR* repressor that also regulates its own expression. (*C*) Simplified model of dose–response in the constructs from *A* and B. ATc (*y*) enters the cell at an influx determined by external ATc concentration (*C*), and leaves through outflux and binding to free TetR molecules (*x*). Free TetR is eliminated by binding to ATc and spontaneous degradation/dilution. TetR affects its own and yEGFP (*z*) production via a repressory Hill function. yEGFP is eliminated through spontaneous degradation/dilution.

grams revealed that at intermediate ATc concentrations, cells switched to the high expression state nonuniformly, giving rise to highly heterogeneous (bimodal) yEGFP expression and high levels of noise (Fig. 2*D*). This represents a potential problem for synthetic gene expression systems that require tight and graded control over a wide range of expression levels (33).

To better understand the experimentally observed behavior of the NR cascade, we developed a computational model based on a biochemical reaction scheme that incorporates both regulator and repressor synthesis [see supporting information (SI) *Appendix* and Figs. S1–S8 for a full description of the model, gene constructs, and controls, and experimental data]. Using this model, we ran stochastic simulations to estimate the gene expression noise for various ATc concentrations. The simulated gene expression mean and noise agreed well with the experimental data (Fig. 2 *A* and *C*). Our simulations suggest that the noise peak at intermediate ATc concentrations is due to high repressor noise, further amplified by the sharp dose–response of the downstream promoter (5) and coupled with slow promoter dynamics (14, 34). In addition, basal expression lowers the noise (5) as the promoter approaches the fully repressed state at ATc = 0. The model also suggests that ATc binds and inactivates free intracellular TetR molecules before interacting with DNA-bound TetR and relieving repression. This gives rise to the sharp increase in dose–response near the lowest ATc concentration that completely depletes free intracellular TetR (Fig. 2*A*).

Transcriptional Cascade with Negative Autoregulation (Linearizer). The computational model allowed us to predict the effect of incorporating feedback into the regulatory part of the cascade. Keeping the reaction rates unchanged, we incorporated regulator self-repression into our model (section 5 in *SI Appendix*), such that the reporter and the repressor were transcribed from identical promoters. Based on published experimental data (32), the only rate change compared with the no-feedback cascade was a 30% decrease in regulator transcription rate at full induction. Stochastic simulations of this modified system predicted a dose–response curve that was linear up to 90% saturation and lower noise levels at all inducer concentrations (Fig. 2 *A–C*).

To verify these computational predictions experimentally, we constructed the linearizer NF cascade by replacing the upstream P_{GAL1} promoter with the $P_{GAL1\text{-}D12}$ promoter, thereby introducing negative autoregulation into the cascade (Fig. 1*B*). Measuring *yEGFP* expression, we indeed observed a linear dose–response ($R^2 = 0.99$, L1-norm $= 6.5 \times 10^{-2}$, see section 6 in *SI Appendix* and Figs. S6, S7 for the definition of these measures and comparison with the NR strain) over a wide range of ATc concentrations, from no induction (0 ng/mL) up to 90% saturation (≈60 ng/mL), confirming our computational predictions (Fig. 2*A*). Flow cytometry over additional low ATc concentrations (starting at 0.1 ng/mL) ruled out nonlinearity in the beginning of the dose–response curve and the possibility that linearity could arise from the leftward shift of a Hill curve (Fig. 2*B* and section 6 in *SI Appendix* and Fig. S8). Furthermore, as predicted computationally, the distribution of *yEGFP* expression in the NF strain was unimodal and narrow, maintaining a low level of noise throughout all inducer concentrations (Fig. 2 *C* and *E*). Compared with earlier findings of noise reduction by NF (20), the effect here is much more pronounced (up to 7-fold at intermediate inducer concentrations).

To verify that reporter gene expression acts as a readout (mimics the dose–response of the upstream regulator, TetR), we also built a single-gene NF system, placing the *tetR*::*yEGFP* fusion construct under the control of $P_{GAL1\text{-}D12}$ promoter. As expected, the dose–response of the single-gene autoregulatory circuit was also linear, and its noise level was comparable with the NF cascade after rescaling (section 2 in *SI Appendix*).

Simple Mathematical Model Explains Linearization and Noise Reduction. After reducing the number of biochemical reactions used for stochastic simulations and assuming mass action kinetics (section 5.3 in *SI Appendix*), we arrived at a set of differential equations that can be used to mathematically explain dose–response linearization in the cascade with NF:

$$\frac{dx}{dt} = aF_x(x) - bxy - dx$$

$$\frac{dy}{dt} = C - bxy - fy \qquad [1]$$

$$\frac{dz}{dt} = aF_z(x) - dz$$

where the variables x, y, and z correspond to free intracellular repressor, inducer, and reporter concentration, respectively, and C is a control parameter proportional to extracellular inducer concentration. Other parameters are a (protein synthesis rate), b (inducer–repressor association rate), d (rate of dilution due to cell growth), and f (combined rate of inducer dilution, outflux, and degradation). Inducer dissociation from the repressor occurs at much slower time scale than the other processes we considered (35), and thus, for the sake of mathematical tractability, it was not included in this model. The functions F_x and F_z describe the repressor dependence of protein synthesis from the upstream and downstream promoters, respectively. Because repression by TetR is generally cooperative (5), we used the

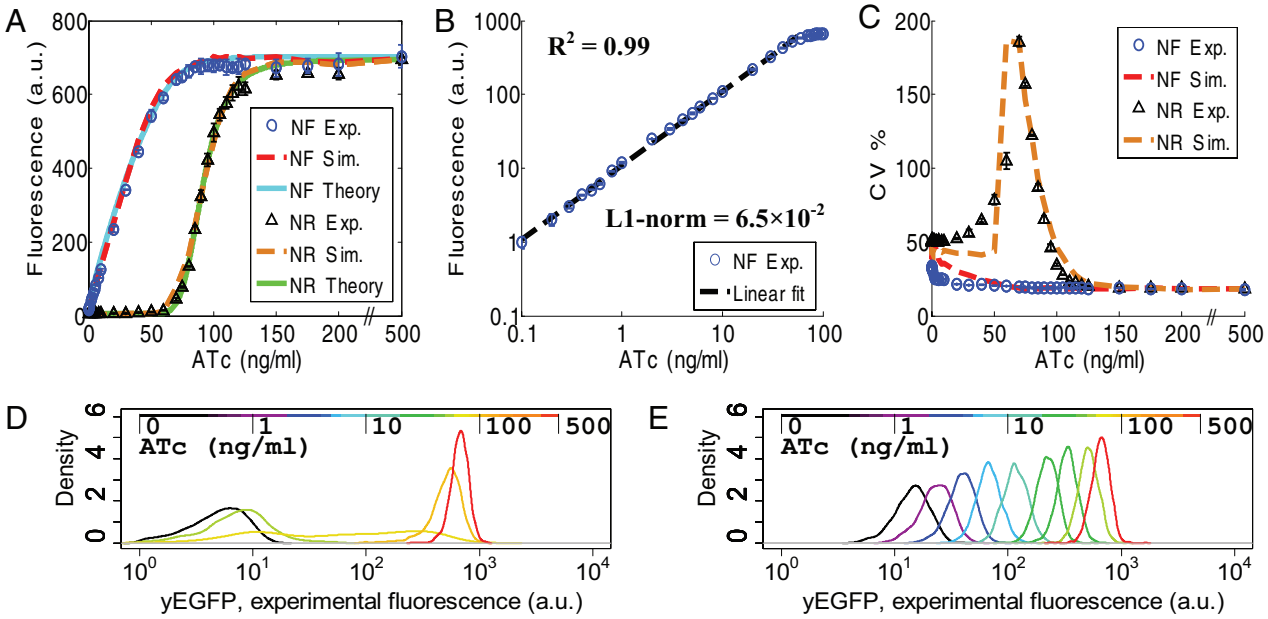

Fig. 2. Linearization and noise reduction due to NF. (*A*) Experimental and simulated dose–response curves for the constructs in Fig. 1. For theoretical curves, the parameters are $a = 50$ nM h^{-1}, $b = 3.6$ nM^{-1} h^{-1}, $C = 0.6$ [ATc] h^{-1}, $d = 0.12$ h^{-1}, $f = 1.2$ h^{-1}, $\theta = 0.44$, $n = 4$, $F_x \equiv 1.5$ for NR strains, and $F_x = F_z$ for NF strains (*B*) Experimental, background-corrected dose–response for the NF cascade and the corresponding linear fit plotted on log–log scale, showing that linearity holds from very small to saturating ATc concentrations (0.1–60 ng/mL). Error bars corresponding to standard deviations (from 3 replicates) are smaller than the symbols. (*C*) Experimentally measured and simulated gene expression noise for the NR and NF gene circuits. (*D* and *E*) Experimental fluorescence histograms for the NR (*D*) and the NF (*E*) strains at increasing ATc concentrations (0–500 ng/mL).

same Hill function to describe the repressor dependence of the 2 identical promoters in the NF strain:

$$F_x(x) = F_z(x) = \frac{\theta^n}{\theta^n + x^n} \qquad [2]$$

where θ is the induction threshold and n is the Hill coefficient. The set of Eqs. **1** also describes the cascade without feedback (NR) after setting $F_x = 1$.

The steady-state solution of Eqs. **1** includes a quasi-linear function $z(C)$, confirming that NF linearizes the dose–response (Fig. 2*A*). This can be understood by considering that below saturation, association with free repressor is the dominant source of decay for both inducer and free repressor, implying that the terms dx and fy are negligible compared with bxy. Therefore, setting $dx \approx fy \approx 0$ in the first 2 equations for the NF strain at steady state results in

$$x = F_x^{-1}\left(\frac{C}{a}\right). \qquad [3]$$

Here, F_x^{-1} is the inverse function of F_x, indicating that x (free repressor concentration) is a predistorted function of C. At the reporter level we obtain

$$z = \frac{a}{d}F_z(x) = \frac{a}{d}F_z\left[F_x^{-1}\left(\frac{C}{a}\right)\right] = \frac{C}{d} \qquad [4]$$

demonstrating that the reporter's promoter redistorts the function $x(C)$, resulting in the linear dependence $z = C/d$. Therefore, provided F_z and F_x are related via a linear transformation

$$F_z(x(C)) = sF_x(x(C + \varphi)) + l \qquad [5]$$

the dose–response will be well approximated by the linear function $z = (sC + s\varphi + l)/d$, where the factors s, l, and φ stretch and move F_x vertically or horizontally (the values $s = 1$, $l = 0$, and $\varphi = 0$ correspond to identical up- and downstream promoters, $F_x \equiv F_z$).

In summary, linearization in the NF cascade requires that the predistortion at the regulator level be redistorted at the reporter level. Therefore, this simple argument predicts a linear dose–response if the repressor dependences F_x and F_z of upstream and downstream promoter activities are related via a linear transformation (section 5.3 in *SI Appendix*).

Linearization of Dose–Response Does Not Depend on the Number of Repressor Sites. To confirm linearization via pre- and redistortion, we constructed 3 additional linearizers (section 4.2 in *SI Appendix* and Figs. S1, S3), using identical up- and downstream promoters with 1 ($P_{GAL1\text{-}S1}$), 2 ($P_{GAL1\text{-}D12}$), or 3 ($P_{GAL1\text{-}T123}$) *tet*O$_2$ sites (32). Importantly, the open-loop (NR) dose-response of the $P_{GAL1\text{-}S1}$ promoter was twice as steep as that of the other two promoters, while the peak noise level increased with the number of *tetO*$_2$ sites in these promoters (32). We combined these promoters in pairs to govern the expression of a *tetR*::*mCherry* fusion as repressor and *yEGFP*::*zeoR* as reporter. As expected, the ATc dependence of gene expression noise and mean in the strain harboring 2 $P_{GAL1\text{-}D12}$ promoters was almost identical to that of the original linearizer after rescaling (sections 3.3 and 4.2 in *SI Appendix* and Fig. S2). More importantly, in accordance with the mathematical prediction that NF linearizes the dose–response if the repressor-dependencies F_z and F_x of up- and downstream promoters are linear transformations of each other, we found that all 3 promoter pairs produced linear dose–responses ($R^2 = 0.99$, L1-norms $= 2.1 \times 10^{-2}$, 5.7×10^{-2}, and 3×10^{-2}, respectively) of nearly identical slopes over a wide range of inducer concentrations, independent of promoter strength, and regardless of the number of *tet*O$_2$ sites present in the promoters.

As a control, we have also replaced the $P_{GAL1\text{-}D12}$ promoter in the original linearizer with different downstream promoters [$P_{GAL1\text{-}S1}$ and $P_{GAL1\text{-}T123}$ (section 4.3 in *SI Appendix*)]. Compar-

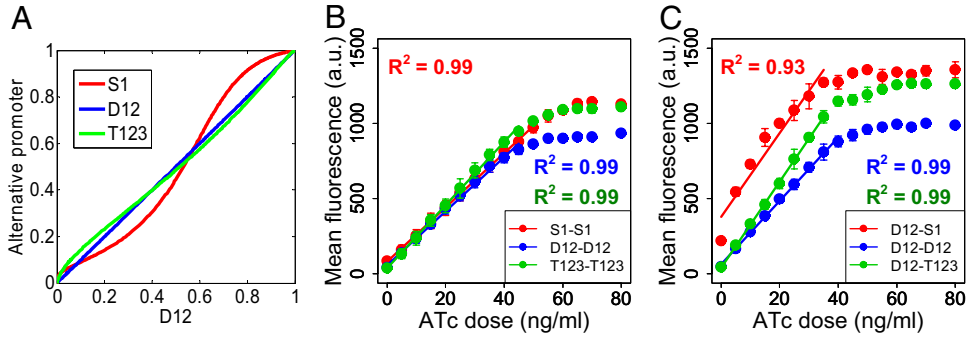

Fig. 3. Confirmation of linearization in alternative NF cascades. (*A*) Linear transformations of best fits to the dose–response curves of $P_{GAL1\text{-}S1}$, $P_{GAL1\text{-}D12}$, and $P_{GAL1\text{-}T123}$ promoters plotted against the $P_{GAL1\text{-}D12}$ promoter, based on the data from ref. 32. (*B*) Experimental dose–response curves and respective linear fits up to saturation levels for 3 different linearizers based on $P_{GAL1\text{-}S1}$ (1 *tet*O_2 site); $P_{GAL1\text{-}D12}$ (2 *tet*O_2 sites); and $P_{GAL1\text{-}T123}$ (3 *tet*O_2 sites). (*C*) Experimental dose–response curves and the corresponding linear fits up to saturation for the NF constructs with $P_{GAL1\text{-}D12}$ promoter upstream and the promoters $P_{GAL1\text{-}S1}$, $P_{GAL1\text{-}D12}$, and $P_{GAL1\text{-}T123}$ downstream, respectively.

ing the dose–response of these downstream promoters to that of $P_{GAL1\text{-}D12}$ in cascades with no feedback (32) we concluded that the repressor dependence of $P_{GAL1\text{-}S1}$ is markedly different, whereas that of $P_{GAL1\text{-}T123}$ is quasi-identical to $P_{GAL1\text{-}D12}$ after linear rescaling (Fig. 3*A*). In accordance with the mathematical prediction, we found by flow cytometry that, compared with the construct with 2 identical $P_{GAL1\text{-}D12}$ promoters, the promoter combination $P_{GAL1\text{-}D12}$–$P_{GAL1\text{-}T123}$ had steeper but still linear dose–response ($R^2 = 0.99$, L1-norm $= 7.9 \times 10^{-2}$), whereas the dose–response of the $P_{GAL1\text{-}D12}$–$P_{GAL1\text{-}S1}$ cascade deviated from linearity ($R^2 = 0.93$, L1-norm $= 14.7 \times 10^{-2}$) (Fig. 3*C* and section 6.2 in *SI Appendix*). This departure from linearity for the latter construct confirms that a NF cascade is a linearizer if the repressor dependencies of upstream and downstream promoters are related via a linear transformation as in Eq. **5**.

Finally, we also observed efficient noise reduction for all promoter combinations with NF (sections 4.2 and 4.3 in *SI Appendix*), suggesting that noise suppression and dose–response linearization are independent properties of our constructs. Overall, these experimental findings confirmed the predictions of the mathematical model, suggesting that linearization in our constructs results from predistortion at the regulator followed by redistortion at the reporter level (Fig. 3).

Discussion

Using a chromosomally integrated gene expression system, we studied the effect of NF on the characteristics of eukaryotic gene expression over a broad range of induction. This is important, because of the "fundamentally different logic of gene regulation" (36) and the different sources and characteristics of gene expression noise in eukaryotes versus prokaryotes (9). Indeed, we observed a massive (7-fold) reduction of noise compared with prokaryotic systems (20) at intermediate induction. Noise reduction at intermediate and high ATc levels might be explained by differences in regulator (free TetR) fluctuations in the 2 different strains (section 5.2.9 in *SI Appendix*).

Importantly, we have also demonstrated that introducing negative autoregulation into a transcriptional cascade can linearize the dose–response before saturation. Currently, no known alternatives exist to linearize the dose–response in eukaryotic gene expression systems. For example, reducing the number of repressor binding sites can result in steeper dose–response, depending on the location of the operator sites (32). Moreover, even when the desired reduction of steepness is obtained, it is accompanied by a drastic increase in basal expression (32). Although to the best of our knowledge, a systematic study of linearization by a gene circuit has not previously been undertaken, similar effects have been widely known and applied in electronics, control theory, and even neuroscience. For example, NF increases the linearity (reduces distortion) in electronic amplifiers, and may play a role in the "spike-frequency adaptation" of neurons (37), converting nonlinear instantaneous firing rate responses to linear at steady state (38).

A set of gene circuits similar to ours have recently been studied in *Escherichia coli* (26), and NF was shown to reduce noise at a wide range of inducer concentrations. However, noise had a U-shaped dependence on inducer concentration in the bacterial construct corresponding to our NF cascade, and there was no noise peak in the bacterial construct corresponding to our NR cascade. The U-shaped inducer dependence of noise was explained by plasmid copy number variation acting as a source of extrinsic noise (7), which is suppressed most efficiently at intermediate inducer concentrations by NF (39). On the other hand, gene copy number variation did not play a role in our single-copy, chromosomally integrated constructs, eliminating this source of extrinsic noise. The presence of a noise peak observed for the NR cascade, and other similar constructs (9, 32, 40), is explained by bimodal yEGFP distributions occurring only at intermediate inducer concentrations, whereas the reporter expression in the corresponding bacterial system was already bimodal even without induction (26). This could be a result of higher *tetR* expression in our constructs, which could increase the steepness of the dose–response curve and shift the induction threshold higher in the absence of feedback. Thus, the specifics of the bacterial and yeast system can account for the different inducer dependence of the gene expression noise and mean in these studies.

The architecture of the linearizer gene circuit closely resembles inducible bacterial operons with repressor control (41) with the exception that bacterial effectors frequently catalyze biochemical reactions or encode transport proteins that affect inducer levels creating additional feedbacks (42). Thus, natural gene circuits with completely identical architecture and linear dose–response might not exist at all. However, the ability of linearizers to convert sigmoidal dose–responses to linear and to eliminate bimodality could have wide-ranging applications for building reliable synthetic transcriptional networks. Based on our results, introducing NF will improve the performance of current gene expression systems by reducing cellular heterogeneity, and by allowing the experimenter to fine-tune the expression of any gene along a linear dose–response curve. This seems particularly important considering the nonlinear dose–response of many artificial transcription activation elements (33), and the wide use of *tet* gene expression systems in bacteria (20, 26, 40), yeast (5, 14, 32), insects (43), and mammalian cells (31). In summary, the precise control of gene expression mean accom-

panied by noise reduction are attractive features that should make the linearizer gene circuit a highly useful tool in synthetic biology.

Materials and Methods

Strains and Media. The haploid *S. cerevisiae* strain YPH500 (α, *ura3-52*, *lys2-801*, *ade2-101*, *trp1Δ63*, *his3Δ200*, *leu2Δ1*) (Stratagene) was used as a parental strain. First, the reporter part of the cascade was integrated into the native *GAL1-GAL10* locus, followed by the integration of regulatory parts into the *ampR* gene of the first integrant. Modified lithium acetate procedure was used for transformation (44). The number of integrations for each construct was verified by PCR and flow cytometry, selecting only the strains with single integrations. Cultures were grown in synthetic drop-out medium with the appropriate supplements to maintain selection (all reagents from Sigma) and supplemented with sugars as described below.

Construction of Cascades. The yeast integrative plasmid pRS4D1 (9, 14) carrying a $P_{GAL1\text{-}D12}$ promoter (pGAL1* in refs. 9 and 14, and D12 in ref. 32) with 2 $tetO_2$ sites and selectable *TRP1* marker was used as the template for all subsequent plasmids in this work. The tetracycline repressor gene (*tetR*) present in the original pRS4D1 plasmid under the control of *GAL10* promoter was replaced with nonfunctional fragment inserted between SacI and SpeI sites. The genetic constructs were then generated in 2 steps. First, in the reporter part, the region of plasmid containing transcriptional terminators flanking $P_{GAL1\text{-}D12}$ promoter and downstream *yEGFP* gene were amplified by PCR and inserted into the pRS403 shuttle vector (Stratagene) between 2 PvuII sites, producing pDN-G1Gh plasmid with *HIS3* selectable marker. Second, in the regulator parts, the functional *tetR* gene was amplified by PCR and placed between BamHI and XhoI sites under the control of either $P_{GAL1\text{-}D12}$ (NF) or P_{GAL1} (NR) promoters, producing the pDN-G1Tt and pDN-NG1Tt plasmids, respectively. The pDN-NG1Tt was engineered, replacing the $P_{GAL1\text{-}D12}$ with the native P_{GAL1} promoter restoring the original sequence between AgeI and BamHI sites, by using the pESC-Leu (Stratagene) as a template. All cloning procedures were performed in *E. coli* XL-10 Gold strain (Stratagene) by using selection by ampicillin (Sigma). All constructs were sequenced in the insert regions with double coverage. Oligonucleotides used in the study can be found in *SI Appendix*.

Flow Cytometry. Single cell colonies were picked from the plate and incubated overnight in synthetic drop-out medium supplemented with glucose 2% at 30 °C. Cell suspension was diluted 1:6, and 100 μL was used to inoculate synthetic drop-out medium supplemented with 2% galactose and increasing concentrations of ATc (0 to 500 ng/mL; ACROS Organics). Cultures were then grown at 30 °C for another 16 h and read on the FACScan flow cytometer (Becton Dickinson) or MoFlo flow cytometer (DAKO North America).

Data Analysis, Computational Models, and Simulations. Flow cytometry data were analyzed using R (R Development Core Team, Vienna). The original log-binned fluorescence intensity values were transformed (by raising 10 to the power of each log bin), and the mean and standard deviation of the resulting values were calculated for each sample within a small forward and side scatter gate to reduce variability in cell size and shape (4). Cells with log fluorescence deviating >3 standard deviations from the geometric mean were considered outliers and were discarded from the analysis. The noise (coefficient of variation) was computed for each sample as the standard deviation divided by the mean. Linearity was assessed by using a linear regression and the L1-norm (see *SI Appendix* for details).

Computational models were developed based on chemical mass action kinetics, and the resulting analytical formulas were fitted in Matlab (MathWorks) to the average of 3 experimental replicates the NR strain by using the fminsearch (Nelder–Mead) algorithm. Stochastic simulations based on the Gillespie algorithm were performed in Dizzy (45) and analyzed with Octave (University of Wisconsin, Madison). The detailed description of the computational model and the sensitivity of the results to various parameters can be found in *SI Appendix* and Table S1.

ACKNOWLEDGMENTS. We thank J. J. Collins (Boston University, Boston) for some of the constructs, yeast strains, and discussions; R. Yu (Molecular Sciences Institute, Berkeley, CA) for the yeast-optimized variant of mCherry; and R. Agarwal, M. Stamatakis, W. Blake, T. F. Cooper, B. Dutta, and G. Shinar for valuable comments and discussions. G.B. was supported by M. D. Anderson Cancer Center start-up funds and K.J. was supported by National Science Foundation Grant DMS-0817649 and a Texas Advanced Research Program/Advanced Technology Program grant. Sequencing was performed at the DNA Analysis core facility; 2-color flow cytometry was done in the Flow Cytometry and Cellular Imaging core facility (both funded by National Cancer Institute Grant CA16672). Some simulations were done on the ''High Performance Computing'' cluster at the M. D. Anderson Cancer Center administered by D. E. Jackson.

1. Rao CV, Wolf DM, Arkin AP (2002) Control, exploitation and tolerance of intracellular noise. *Nature* 420:231–237.
2. Raser JM, O'Shea EK (2005) Noise in gene expression: Origins, consequences, and control. *Science* 309:2010–2013.
3. Kaern M, Elston TC, Blake WJ, Collins JJ (2005) Stochasticity in gene expression: From theories to phenotypes. *Nat Rev Genet* 6:451–464.
4. Newman JR, et al. (2006) Single-cell proteomic analysis of *S. cerevisiae* reveals the architecture of biological noise. *Nature* 441:840–846.
5. Becskei A, Kaufmann BB, van Oudenaarden A (2005) Contributions of low molecule number and chromosomal positioning to stochastic gene expression. *Nat Genet* 37:937–944.
6. Samoilov MS, Price G, Arkin AP (2006) From fluctuations to phenotypes: The physiology of noise. *Sci STKE* 2006:re17.
7. Elowitz MB, Levine AJ, Siggia ED, Swain PS (2002) Stochastic gene expression in a single cell. *Science* 297:1183–1186.
8. Ozbudak EM, et al. (2002) Regulation of noise in the expression of a single gene. *Nat Genet* 31:69–73.
9. Blake WJ, Kaern M, Cantor CR, Collins JJ (2003) Noise in eukaryotic gene expression. *Nature* 422:633–637.
10. Rosenfeld N, et al. (2005) Gene regulation at the single-cell level. *Science* 307:1962–1965.
11. Colman-Lerner A, et al. (2005) Regulated cell-to-cell variation in a cell-fate decision system. *Nature* 437:699–706.
12. Fraser HB, et al. (2004) Noise minimization in eukaryotic gene expression. *PLoS Biol* 2:e137.
13. Maamar H, Raj A, Dubnau D (2007) Noise in gene expression determines cell fate in *Bacillus subtilis*. *Science* 317:526–529.
14. Blake WJ, et al. (2006) Phenotypic consequences of promoter-mediated transcriptional noise. *Mol Cell* 24:853–865.
15. Guelzim N, Bottani S, Bourgine P, Kepes F (2002) Topological and causal structure of the yeast transcriptional regulatory network. *Nat Genet* 31:60–63.
16. Shen-Orr SS, Milo R, Mangan S, Alon U (2002) Network motifs in the transcriptional regulation network of *Escherichia coli*. *Nat Genet* 31:64–68.
17. Thieffry D, Huerta AM, Perez-Rueda E, Collado-Vides J (1998) From specific gene regulation to genomic networks: A global analysis of transcriptional regulation in *Escherichia coli*. *BioEssays* 20:433–440.
18. Stekel DJ, Jenkins DJ (2008) Strong negative self regulation of prokaryotic transcription factors increases the intrinsic noise of protein expression. *BMC Syst Biol* 2:6.
19. Thattai M, van Oudenaarden A (2001) Intrinsic noise in gene regulatory networks. *Proc Natl Acad Sci USA* 98:8614–8619.
20. Becskei A, Serrano L (2000) Engineering stability in gene networks by autoregulation. *Nature* 405:590–593.
21. Austin DW, et al. (2006) Gene network shaping of inherent noise spectra. *Nature* 439:608–611.
22. Rosenfeld N, Elowitz MB, Alon U (2002) Negative autoregulation speeds the response times of transcription networks. *J Mol Biol* 323:785–793.
23. Elowitz MB, Leibler S (2000) A synthetic oscillatory network of transcriptional regulators. *Nature* 403:335–338.
24. Stricker J, et al. (2008) A fast, robust and tunable synthetic gene oscillator. *Nature* 456:516–519.
25. Batchelor E, Silhavy TJ, Goulian M (2004) Continuous control in bacterial regulatory circuits. *J Bacteriol* 186:7618–7625.
26. Dublanche Y, et al. (2006) Noise in transcription negative feedback loops: Simulation and experimental analysis. *Mol Syst Biol* 2:41.
27. Guido NJ, et al. (2006) A bottom-up approach to gene regulation. *Nature* 439:856–860.
28. Bio FAB Group (2006) Engineering life: Building a fab for biology. *Sci Am* 294(6):44–51.
29. Rosenfeld N, et al. (2007) Accurate prediction of gene feedback circuit behavior from component properties. *Mol Syst Biol* 3:143.
30. Gardner TS, Cantor CR, Collins JJ (2000) Construction of a genetic toggle switch in *Escherichia coli*. *Nature* 403:339–342.
31. Berens C, Hillen W (2003) Gene regulation by tetracyclines. Constraints of resistance regulation in bacteria shape TetR for application in eukaryotes. *Eur J Biochem* 270:3109–3121.
32. Murphy KF, Balázsi G, Collins JJ (2007) Combinatorial promoter design for engineering noisy gene expression. *Proc Natl Acad Sci USA* 104:12726–12731.
33. Kramer BP, Weber W, Fussenegger M (2003) Artificial regulatory networks and cascades for discrete multilevel transgene control in mammalian cells. *Biotechnol Bioeng* 83:810–820.
34. Raser JM, O'Shea EK (2004) Control of stochasticity in eukaryotic gene expression. *Science* 304:1811–1814.
35. Schubert P, Pfleiderer K, Hillen W (2004) Tet repressor residues indirectly recognizing anhydrotetracycline. *Eur J Biochem* 271:2144–2152.
36. Struhl K (1999) Fundamentally different logic of gene regulation in eukaryotes and prokaryotes. *Cell* 98:1–4.

37. Gabbiani F, Krapp HG (2006) Spike-frequency adaptation and intrinsic properties of an identified, looming-sensitive neuron. *J Neurophysiol* 96:2951–2962.
38. Ermentrout B (1998) Linearization of F-I curves by adaptation. *Neural Comput* 10:1721–1729.
39. Paulsson J (2004) Summing up the noise in gene networks. *Nature* 427:415–418.
40. Hooshangi S, Thiberge S, Weiss R (2005) Ultrasensitivity and noise propagation in a synthetic transcriptional cascade. *Proc Natl Acad Sci USA* 102:3581–3586.
41. Wall ME, Hlavacek WS, Savageau MA (2004) Design of gene circuits: Lessons from bacteria. *Nat Rev Genet* 5:34–42.
42. Savageau MA (1974) Comparison of classical and autogenous systems of regulation in inducible operons. *Nature* 252:546–549.
43. Bello B, Resendez-Perez D, Gehring WJ (1998) Spatial and temporal targeting of gene expression in *Drosophila* by means of a tetracycline-dependent transactivator system. *Development* 125:2193–2202.
44. Gietz RD, Schiestl RH, Willems AR, Woods RA (1995) Studies on the transformation of intact yeast cells by the LiAc/SS-DNA/PEG procedure. *Yeast* 11:355–360.
45. Ramsey S, Orrell D, Bolouri H (2005) Dizzy: Stochastic simulation of large-scale genetic regulatory networks. *J Bioinform Comput Biol* 3:415–436.